

CHAPTER XV

The first high resolution spectrum of gas phase cyclopropyl radical

15.1 Introduction

Similar to the previous radical studies presented in this thesis, a general interest in the ubiquitously important hydrocarbon radicals motivates our study of cyclopropyl ($\text{CH}_2\text{-CH-CH}_2$). Particular to cyclopropyl, however, are properties arising from its simple cyclic structure (see Figure 15.1). With only three carbons, this molecule is an important prototype for “ring strain”. Furthermore, as illustrated in the top of Figure 15.1, the absence of a “sixth” hydrogen (which would make cyclopropane) results in a unique tunneling pathway, whereby the lone hydrogen tunnels through the radical center. Additionally, spectroscopic characterization of cyclopropyl, coupled with detailed spectral analysis of the more stable isomer allyl (see Chapter 12), are steps towards possible quantum-state resolved kinetic studies of unimolecular ring opening/closing (see bottom of Figure 15.1).

The presence of the more stable allyl isomer (ab-initio $\Delta E = 33$ kcal/mol for conversion from allyl to cyclopropyl)^{1,2} further complicates the task of generating sufficient densities for experimental detection.³ The first successful

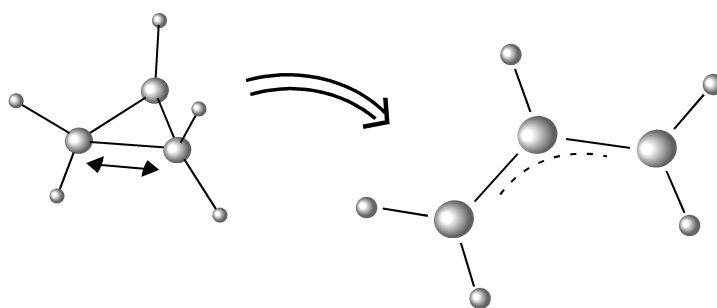
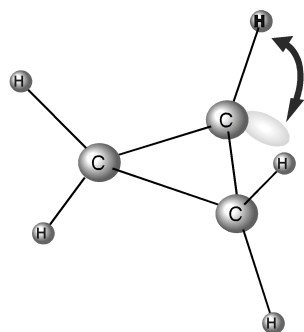


Figure 15.1 Two of the dynamical motivations for studying cyclopropyl radical, tunneling of the lone hydrogen through the radical center (top) and the possibility of unimolecular ring opening to form allyl (bottom).

detection was reported by Fessenden and Schuler, who recorded the electron spin resonance (ESR) spectrum of cyclopropyl prepared in liquid cyclopropane irradiated by an electron beam from a Van der Graff accelerator.⁴ This ESR spectrum, along with subsequent ESR studies,⁵ provided the nuclear hyperfine parameters. The photoelectron spectrum of cyclopropyl was obtained by Dyke et al.⁶ by reacting cyclopropane with fluorine atoms in the gas phase. Finally, and most relevant to the current work, the infrared absorption spectrum of cyclopropyl

trapped in a cryogenic Ar matrix (obtained by irradiating trapped allyl radical with 410 nm light to promote ring closure) was reported by Holtzhauer et al.² in 1990. While these heroic efforts have provided considerable information, the lack of a rotationally resolved spectrum has limited even basic structural characterization.

This relative paucity of experimental studies is not reflected in the number of theoretical studies.^{1-3,7-12} While most of the theoretical efforts have been directed toward elucidating the ESR spectra, often reports are also ab-initio geometries and even vibrational frequencies.^{1-3,7} These theoretical estimates can provide a valuable starting point for a high resolution spectroscopic search.

Presented in this chapter is the first high-resolution detection of gas phase cyclopropyl radical. Fitting of the spectrum to an asymmetric top Hamiltonian provides both the vibrational origin and rotational constants. The vibrational origin is directly compared with the theoretical estimates and the rotational constants are compared with rotational constants calculated from ab-initio geometries. Splitting of the spectrum into two separate bands due to the tunneling motion is also observed and discussed.

15.2 Experiment

The jet cooled cyclopropyl radical is generated by expanding trace quantities of cyclopropyl-bromide (0.2 %) in first run Ne (70% Ne, 30% He) through our slit-jet discharge source. Typical backing pressures are 400 Torr, with peak discharge currents of ≈ 1 Amp. The IR detection is exactly the same as

described in previous chapters, with precursor discrimination accomplished via the discharge on/discharge off technique presented in Chapter 13. This data was recorded prior to the development of the concentration modulation technique described in Chapter 10, and therefore the signal to noise presented could be substantially improved upon.

15.3 Results and analysis

Cyclopropyl radical contains five C-H bonds and therefore five vibrational frequencies that lie in the infrared region: the lone C-H stretch, and the in-phase and out-of-phase symmetric and antisymmetric CH₂ stretches. Out of these five only three are infrared active, i.e., possess nonzero dipole moment derivatives, namely, the lone C-H stretch, the in-phase antisymmetric stretch, and the out-of-phase symmetric stretch. Both ab-initio calculations and the matrix isolation spectra suggest the lone C-H stretch and the in-phase antisymmetric stretch to be the most intense. Since predicted frequencies for both of these vibrations lie to the blue of the symmetric CH₂ stretch, covering the from 3040 cm⁻¹ to 3120 cm⁻¹, we performed continuous high resolution, high sensitivity scans from 3125 to 3030 cm⁻¹.

Displayed in Figure 15.2 is the central Q-branch of a weak band observed near 3040 cm⁻¹. Corresponding P and R-branches are also observed, and an assignment to a C-type band, consistent with the in-phase antisymmetric CH₂ stretch, is made. The transition frequencies, listed in Table 15.1, are fit to a

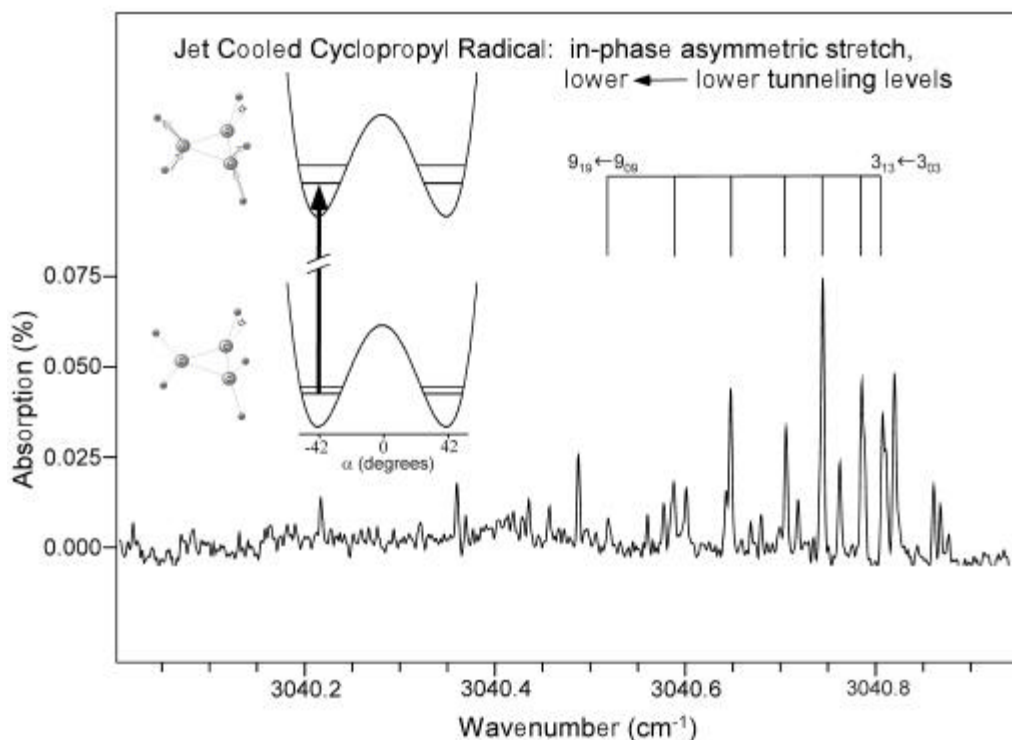


Figure 15.2 A section of the spectral scan displaying the Q-branch structure for the lower←lower vibrational band of cyclopropyl radical.

standard *A*-reduction Watson Hamiltonian, using the III R representation, appropriate for an asymmetric top. The results of the fit are presented in Table 15.2. It is worth noting that while the standard deviation of the fit is ≈ 90 MHz it is still approximately an order of magnitude worse than the frequency precision. Since we have only conducted one scan over this region it is premature to attribute this discrepancy to either low signal to noise or rotational perturbations. The vibrational assignment to the in-phase antisymmetric CH₂ stretch is based on

Table 15.1 Observed transition frequencies for the $v = 1 \leftarrow 0$ in phase asymmetric CH_2 stretch transition in cyclopropyl ($\text{CH}_2 - \text{CH} - \text{CH}_2$) radical. These transitions connect the lower \leftarrow lower tunneling levels.

$J_{K^a, K^c} \leftarrow J_{K^a, K^c}^2$	Wavenumber (cm^{-1})	$J_{K^a, K^c} \leftarrow J_{K^a, K^c}^2$	Wavenumber (cm^{-1})
$4_{4,1} \leftarrow 5_{5,1}$	3033.0666	$4_{1,4} \leftarrow 4_{0,4}$	3040.7802
$4_{4,0} \leftarrow 5_{5,0}$	3033.0882	$2_{1,2} \leftarrow 2_{0,2}$	3040.8557
$4_{3,2} \leftarrow 5_{4,2}$	3033.3115	$2_{2,1} \leftarrow 2_{1,1}$	3041.1393
$4_{1,3} \leftarrow 5_{2,3}$	3033.4975	$3_{2,2} \leftarrow 3_{1,2}$	3040.9259
$4_{2,2} \leftarrow 5_{3,2}$	3033.5862	$1_{1,1} \leftarrow 1_{0,1}$	3040.9462
$3_{3,1} \leftarrow 4_{4,1}$	3034.6426	$5_{2,4} \leftarrow 5_{1,4}$	3040.7391
$3_{1,3} \leftarrow 4_{2,3}$	3034.9174	$4_{2,3} \leftarrow 4_{1,3}$	3040.8026
$3_{0,3} \leftarrow 4_{1,3}$	3034.9404	$4_{1,3} \leftarrow 4_{2,3}$	3040.7391
$3_{1,2} \leftarrow 4_{2,2}$	3035.0333	$3_{2,2} \leftarrow 3_{1,2}$	3040.9259
$2_{2,1} \leftarrow 3_{3,1}$	3036.2129	$3_{3,1} \leftarrow 3_{2,1}$	3041.4383
$2_{2,0} \leftarrow 3_{3,0}$	3036.2852	$3_{2,1} \leftarrow 3_{3,1}$	3040.1840
$2_{0,2} \leftarrow 3_{1,2}$	3036.4679	$1_{1,0} \leftarrow 0_{0,0}$	3042.3242
$2_{1,1} \leftarrow 3_{2,1}$	3036.5048	$2_{1,1} \leftarrow 1_{0,1}$	3043.6843
$1_{1,1} \leftarrow 2_{2,1}$	3037.7679	$2_{2,0} \leftarrow 1_{1,0}$	3043.8232
$1_{1,0} \leftarrow 2_{2,0}$	3037.8433	$2_{2,1} \leftarrow 1_{1,1}$	3043.9026
$1_{0,1} \leftarrow 2_{1,1}$	3037.9687	$3_{2,1} \leftarrow 2_{1,1}$	3045.1085
$0_{0,0} \leftarrow 1_{1,0}$	3039.3643	$3_{1,2} \leftarrow 2_{0,2}$	3045.1454
$10_{1,0} \leftarrow 10_{2,0}$	3040.4301	$3_{2,2} \leftarrow 2_{1,2}$	3045.2458
$9_{0,9} \leftarrow 9_{1,9}$	3040.5139	$3_{3,0} \leftarrow 2_{2,0}$	3045.3659
$8_{1,8} \leftarrow 8_{0,8}$	3040.5825	$3_{3,1} \leftarrow 2_{2,1}$	3045.4403
$8_{0,8} \leftarrow 8_{1,8}$	3040.5825	$4_{2,2} \leftarrow 3_{1,2}$	3046.4980
$7_{2,6} \leftarrow 7_{1,6}$	3040.6376	$4_{3,1} \leftarrow 3_{2,1}$	3046.5566
$7_{0,7} \leftarrow 7_{1,7}$	3040.6424	$4_{3,2} \leftarrow 3_{2,2}$	3046.7324
$7_{1,7} \leftarrow 7_{0,7}$	3040.6424	$4_{4,0} \leftarrow 3_{3,0}$	3046.9390
$6_{2,5} \leftarrow 6_{1,5}$	3040.6744		
$6_{1,6} \leftarrow 6_{0,6}$	3040.7005		
$6_{0,6} \leftarrow 6_{1,6}$	3040.7005		
$5_{0,5} \leftarrow 5_{1,5}$	3040.7391		
$5_{1,5} \leftarrow 5_{0,5}$	3040.7391		
$4_{0,4} \leftarrow 4_{1,4}$	3040.7802		

Table 15.2 Spectroscopic constants (in cm^{-1}) determined from fits of the transition frequencies to an *A*-reduction Watson Hamiltonian using the III R representation. The uncertainties in parentheses represent one standard deviation in the units of the last reported digit.

	Lower Tunneling \leftarrow Lower Tunneling	
	$\nu = 0$	$\nu = 1$
<i>A</i>	0.79335(30)	0.79288(30)
<i>B</i>	0.69108(31)	0.68474(30)
<i>C</i>	0.452(35)	0.449(36)
$D_J \times 10^5$	1.96(83)	2.05(89)
$D_{JK} \times 10^5$	7.7(46)	8.1(45)
ν_0	3040.8458(12)	
σ	3.1×10^{-3}	

both the band type, and comparison with both ab-initio calculations and the matrix isolation data.

In addition to the vibrational assignment, the tunneling of the lone hydrogen through the radical center splits the energy levels into pairs. We must therefore assign both the ground and vibrationally excited tunneling level (i.e., upper or lower). This is facilitated by considering the nuclear spin statistics. Cyclopropyl radical posses two pairs of identical spin $\frac{1}{2}$ hydrogen nuclei. The total wavefunction, which may be expressed as a product of the electronic, vibrational, tunneling, rotational, and nuclear spin wavefunction,

$$\Psi_{tot} = \Psi_{electronic} \Psi_{vib} \Psi_{tunneling} \Psi_{rotational} \Psi_{nuclear-spin} \quad (15.1)$$

must be symmetric with respect to a 180° rotation about the b molecular axis (i.e. the motion which exchanges identical nuclei). The symmetries of the different components of the wavefunction (w.r.t. that 180° rotation) may be assigned as follows:

$$\Psi_{electronic} = -1$$

$$\Psi_{vibrational} = 1 \quad (\text{ground state})$$

$$\Psi_{vibrational} = -1 \quad (\text{excited state})$$

$$\Psi_{tunneling} = 1 \quad (\text{ground state})$$

$$\Psi_{tunneling} = -1 \quad (\text{excited state})$$

$$\Psi_{rotation} = 1 \quad (k_a + k_c = \text{even})$$

$$\Psi_{rotation} = -1 \quad (k_a + k_c = \text{odd})$$

$$\Psi_{nuclear-spin} = 1 \quad (\text{spin weight} = 10 \quad)$$

$$\Psi_{nuclear-spin} = -1 \quad (\text{spin weight} = 6 \quad)$$

Since the total product must equal one, to satisfy exchange symmetries, in order for transitions to originate from the lower tunneling level, transitions from levels with $k_a+k_c = \text{odd}$ must be strong and vice versa. Displayed in Figure 15.3 is a section of the experimentally observed R-branch and simulations for the lower and upper tunneling level. This vibrational band is therefore assigned to transitions originating from the lower tunneling level, due to the improved agreement with intensity alternations. Furthermore, from a combination of i)

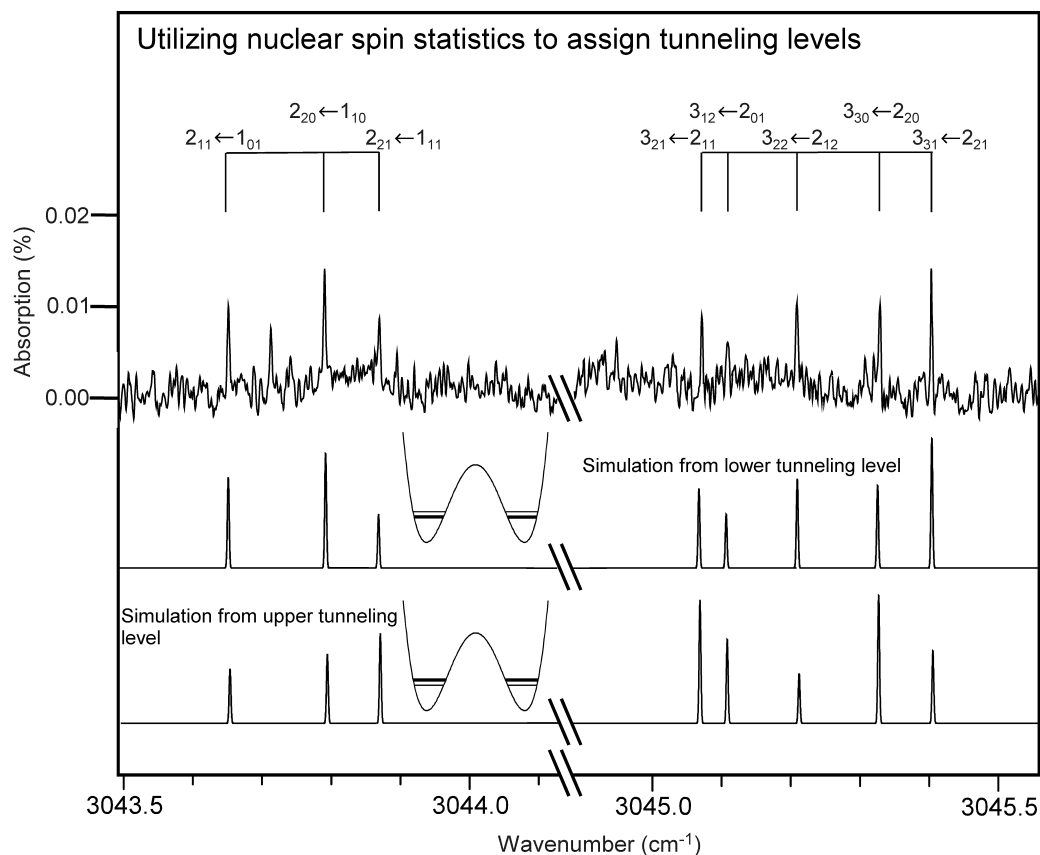


Figure 15.3 Displaying how nuclear spin statistics can be utilized to assign the tunneling level

restrictions of nuclear spins, ii) inability for an IR photon to flip nuclear spin, and iii) selection rules for a c-type transition, the vibrationally excited state tunneling level can also be assigned to the lower (i.e. c-type bands result in lower←lower and upper←upper tunneling transitions).

A consequence of this analysis is the prediction that transitions out of the upper tunneling level should also be observed, though perhaps weaker due to cooling in the expansion. Displayed in Figure 15.4 is another, though weaker, Q-branch which we assign to transitions out of the upper tunneling level. No P or R branch transitions have been assigned, due to the low signal to noise, and

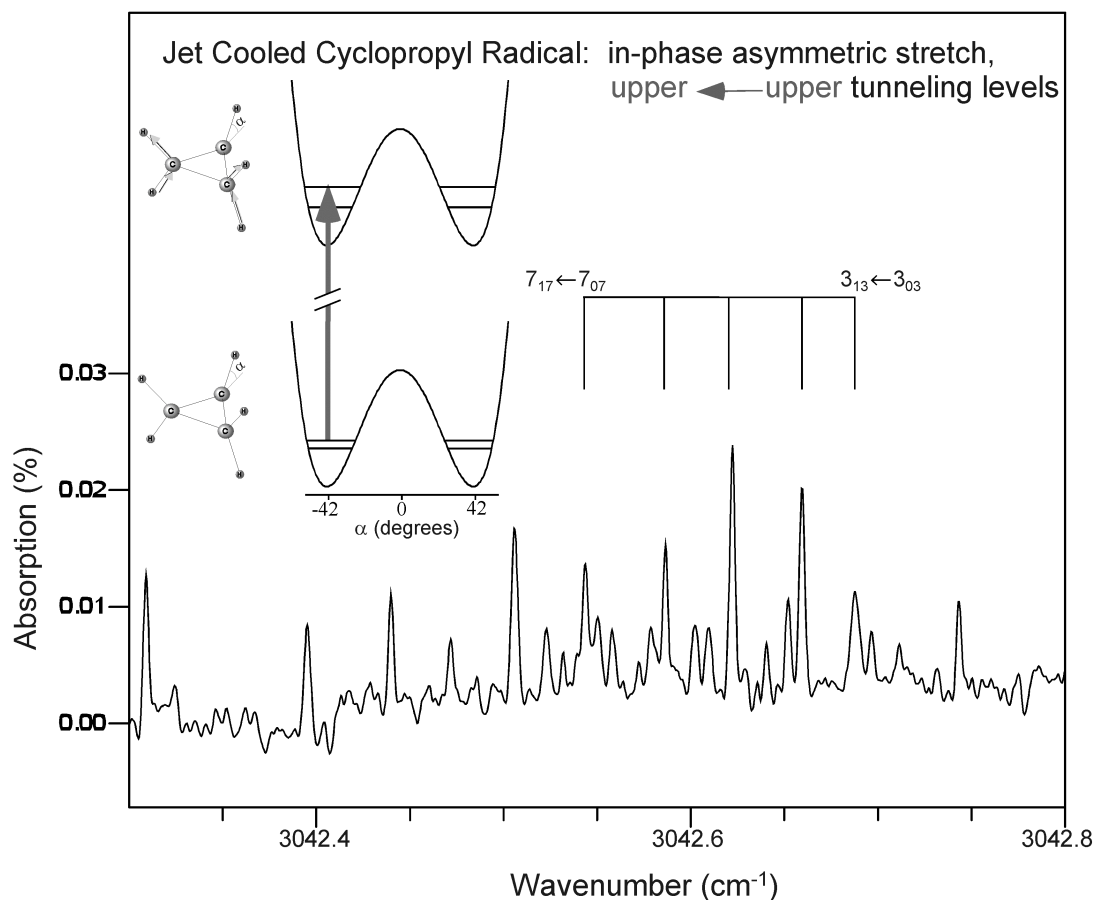


Figure 15.4 A section of the spectrum displaying the Q-branch for the upper←upper tunneling transitions in cyclopropyl.

therefore no spectroscopic fit has been attempted. The origin of this Q-branch is approximately 1.8 cm^{-1} to the blue of the lower←lower band origin. This would correspond to an increase in the tunneling splitting upon vibrational excitation by this amount. Theoretical estimates for the ground state predict a $\approx 1 \text{ cm}^{-1}$ tunneling splitting,⁷ which if correct would correspond to a large fractional effect due to vibrational excitation. A crude experimental estimate is provided by the observed ≈ 2.6 intensity ratio of these two Q-branches. Assuming thermal,

Boltzmann equilibration, for the 15 K temperature in the jet the observed intensity ration would correspond to an approximate 10 cm^{-1} tunneling splitting, i.e. one order of magnitude more facile than theoretically predicted.

15.4 Discussion

One of the benefits associated with measurements in the gas phase is that a direct comparison can be made to theoretical predictions without worry of environmental effects. Displayed in Table 15.3 is such a comparison. The theoretical values^{1,3,7} are based on scaled harmonic predictions, where the scaling factor was obtained via identical calculations on cyclopropane. The theoretical estimates for rotational constants are produced via diagonalization of the moment of inertia tensor for each reported equilibrium geometry. Also included for comparison in the table is the matrix value.² The good qualitative agreement, especially with the matrix value, further corroborates the assignment of this spectrum to cyclopropyl.

Table 15.3 Comparison between the theoretical ab-initio estimates, the matrix value, and the gas phase value presented in this chapter for cyclopropyl vibrational energy and rotational constants. All values are in cm^{-1} . The theoretical rotational constants were calculated from the ab-initio geometries.

	Vibrational Energy	Rotational Constant		
		A	B	C
Ref 3	3073	0.7895	0.6834	0.4409
Ref 1	3066	0.8021	0.6956	0.4472
Ref 8	3084	0.7908	0.6838	0.4410
Matrix	3049	---	---	---
This work	3040.8458(12)	0.79335(30)	0.69108(31)	0.452(35)

15.5 Future directions

One obvious avenue to exploit is the improved noise suppression provided by the concentration modulation technique. Increased signal to noise would not only minimize ambiguities in the assigned spectrum, but permit an observation and assignment of P and R-branch transitions for the upper \leftarrow upper tunneling band. Since one of the motivations for undergoing high resolution studies of cyclopropyl is to discern the timescale for the tunneling motion, a direct spectroscopic measurement of that quantity is therefore desired. This would in principle be provided by the lone C-H stretch, which is predicted to be a hybrid band, i.e., both b and c-type bands should be observed. Since the tunneling selection rules differ for the two band types (for b-type upper \leftarrow lower and lower \leftarrow upper) observation of both would provide a precise measurement of the tunneling splittings. Preliminary spectral searches over the predicted lone C-H stretch region revealed extremely weak ($S/N \approx 2$) transitions. Again, the improved noise suppression provided by the concentration modulation technique would help.

References for Chapter 15

- 1 C. Cometta-Morini, T. K. Ha, and J. F. M. Oth, *Journal of Molecular Structure (Theochem)* **188**, 79-94 (1989).
- 2 K. Holtzhauer, C. Cometta-Morini, and J. F. M. Oth, *Journal of Physical Organic Chemistry* **3**, 219-229 (1990).
- 3 M. J. Dupuis and J. Pacansky, *Journal of Chemical Physics* **76**, 2511-2515 (1982).
- 4 R. W. Fessenden and R. H. Schuler, *Journal of Chemical Physics* **39**, 2147-2195 (1963).
- 5 L. J. Johnston and K. U. Ingold, *Journal of the American Chemical Society* **108**, 2343-2348 (1986).
- 6 J. Dyke, A. Ellis, N. Jonathan, and A. Morris, *Journal of The Chemical Society, Faraday Transactions* **2**, 1573-1586 (1985).
- 7 V. Barone, C. Minichino, H. Faucher, R. Subra, and A. Grand, *Chemical Physics Letters* **205**, 324-330 (1993).
- 8 V. Barone, C. Adamo, Y. Brunel, and R. Subra, *Journal of Chemical Physics* **105**, 3168-3174 (1996).
- 9 V. Barone and R. Subra, *Journal of Chemical Physics* **104**, 2630-2637 (1996).
- 10 K. Ohta, H. Nakatsuji, K. Hirao, and T. Yonezawa, *Journal of Chemical Physics* **73**, 1770-1776 (1980).
- 11 Y. Ellinger, R. Subra, B. Levy, P. Millie, and G. Berthier, *Journal of Chemical Physics* **62**, 10-29 (1975).
- 12 M. H. Lien and A. C. Hopkinson, *Journal of Computational Chemistry* **6**, 274-281 (1985).